INSTITUTE OF PHYSICS PUBLISHING NANOTECHNOLOGY
Nanotechnology **16** (2005) 583–589 doi:10.1088/0957-4484/16/4/041

Chaotic signature in the motion of coupled carbon nanotube oscillators

V R Coluci[1], S B Legoas[2], M A M de Aguiar[1] and D S Galvão[1]

[1] Instituto de Física 'Gleb Wataghin', Universidade Estadual de Campinas, CP 6165, 13083-970 Campinas SP, Brazil
[2] Departamento de Física, Universidade Federal do Amazonas, 69077-000 Manaus AM, Brazil

E-mail: coluci@ifi.unicamp.br

Received 17 November 2004, in final form 12 January 2005
Published 1 March 2005
Online at stacks.iop.org/Nano/16/583

Abstract
The motion of coupled oscillators based on multiwalled carbon nanotubes is studied using rigid-body dynamics simulations. The results show the existence of chaotic and regular behaviours for a given total energy, indicating the manifestation of chaos in nanoscaled mechanical systems based on carbon nanotube oscillators. Different regular motions are observed for different total energies, and they can be obtained by appropriately choosing the initial conditions. This possibility can allow the construction of multi-functional nano-devices based on multiwalled carbon nanotube oscillators.

M This article features online multimedia enhancements

1. Introduction

It has become common knowledge that multiwalled carbon nanotubes (MWNTs) [1] represented a breakthrough in nanotechnology [2]. New and exciting phenomena have been observed in these systems [3], including field emission [4], quantum conductance [5], constant-force nanosprings [6], as well as proposals for MWNT-based nano-devices [7]. High-resolution transmission electron microscopy (HRTEM) experiments involving MWNTs have demonstrated an ultra-low friction telescopic extension of MWNTs, opening up the possibility of building new kinds of nano-devices such as linear bearings [6] and nano-oscillators [7].

Analyzing a slightly modified configuration of the HRTEM experiments of Cumings and Zettl [6], Zheng and Jiang [7] have proposed an MWNT-based mechanical oscillator which could oscillate at gigahertz range. The oscillation mechanism is due to the excess of the van der Waals potential energy which leads to a restoring force acting on the MWNT core and causing its retraction to the equilibrium position [8]. Several studies involving double-walled carbon nanotubes have been carried out in order to investigate the operation of such nanotube-based devices [9–16].

An application of carbon nanotube oscillators as building blocks for nanoscale engines has been investigated by Kang and Hwang using molecular dynamics simulations [17]. They have analysed the integration of different nano-devices and their respective functionalities to simulate the operation of a nanoscale engine based on carbon nanotube oscillators. This approach creates the possibility of using integrated carbon nanostructures in the design of nano-engineering machines.

The goals of the present work are to propose and study a modification of the carbon nanotube oscillator configuration [7] in order to allow the movement of more than one tube. This new configuration can be seen as two coupled carbon nanotube oscillators and represents a new building block type for nano-machines. We have demonstrated that chaotic and regular movements can appear in such a configuration.

It is well known that oscillator based configurations, such as the Duffing oscillator and the double pendulum, can exhibit chaotic behaviours. The irregular behaviour of many physical systems has been the subject of intense experimental and theoretical investigations [18, 19]. Chaotic manifestations can appear in systems with different size scales, from the quantum domain (the behaviour of a hydrogen atom in an oscillating electric field [20–22]) to stellar dimensions with, for instance, the motion of a relativistic three-body self-gravitating system [23]. The system of two coupled carbon nanotube oscillators investigated in this work is an example of a nanoscaled configuration which can exhibit chaotic behaviour.

 © 2005 IOP Publishing Ltd Printed in the UK

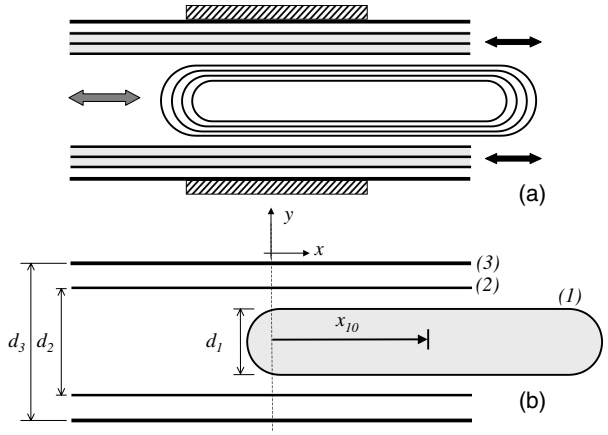

Figure 1. (a) Schematic representation of a multiwalled carbon nanotube composed of one fixed outer tube, one moveable four-shell core and three inner tubes. (b) The simplest case of (a) where the oscillator is formed by a one-shell core (1), one inner (2), and one outer (3) tube with diameters d_1, d_2, and d_3, respectively. For this case the centre of mass of the core is located at the distance x_{10} from the reference system origin.

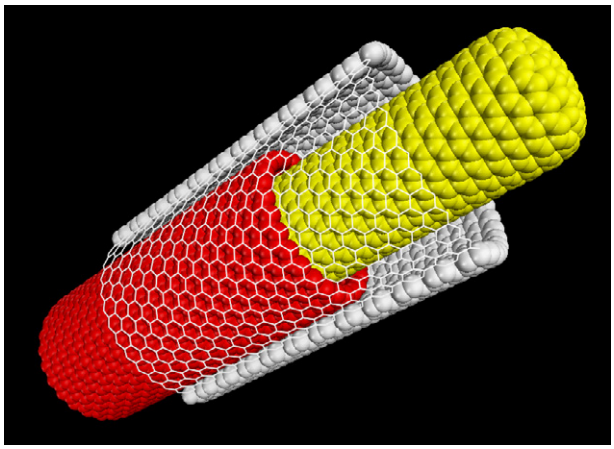

Figure 2. Atomistic view of a triple-walled carbon nanotube. If the outer tube (white) is fixed, the moveable core (yellow/light grey) and inner tube (red/dark grey) can be viewed as two coupled oscillators. (This figure is in colour only in the electronic version)

2. Coupled carbon nanotube oscillators

Oscillators based on MWNTs are formed by a combination of capped and non-capped n concentric tubes. The model considered in this work (figure 1) is an extension of the configuration proposed by Zheng and Jiang [7]. In our system the fixed part is the l outermost tubes, and the remaining tubes are divided into a k-shell core, and n–k–l inner tubes (figure 1(a)). In the particular case of HRTEM experiments [6], an $n = 9$ and $k = 4$ tube configuration has been investigated. On the other hand, the theoretical works involving carbon nanotube oscillators [9–16] have mainly focused on a double-walled system, i.e., $n = 2$, $k = 1$, and $l = 1$. In this case, it is only one tube (core) that can move under the effect of one fixed outer tube.

However, in principle, for oscillators based on MWNTs with $n > 2$ and $k \geqslant 1$, the inner tubes could also move and interact with the core, disturbing its movement. The purpose of this work is to study of the effects of moveable inner tubes in the oscillation behaviour of MWNT oscillators. We have investigated the motion of a triple-walled carbon nanotube oscillator (figure 1(b)) and determined the types of motions that this system can exhibit. This is the simplest case ($n = 3$, $k = 1$, and $l = 1$) of the figure 1(a), where the outer tube is fixed and the core and the inner tube can be viewed as two coupled oscillators. An atomistic view of such a configuration is shown in figure 2. Experimentally, triple-walled carbon nanotubes can be obtained by catalytic chemical vapour deposition processes; see for instance [24].

3. Methodology

We consider a system of three rigid tubes perfectly coupled in the radial direction where the moveable tubes (core and inner tube) can move only in the x direction (figure 1(b)). The total energy E is assumed to be conserved and we have not considered any type of rotation. This approach has also been used by Zheng *et al* [8] for determining the oscillation frequency expression for carbon nanotube oscillators, and by Sohlberg *et al* [25] in the study of molecular bearings. Sohlberg *et al* [25] have also shown that this approximation can accurately model nanosystems operating in low temperatures, reproducing the essentials of their dynamics.

Within this approximation vibrational effects due to the thermal motion of the atoms are neglected. These effects have been shown to be important to the friction phenomenon [12, 15]. Tangney *et al* have shown that when the timescale of the relative motion between the tubes is comparable to the thermal vibrations of the atoms the friction force is strongly nonlinear ($\propto |v|^2$, where v is the relative velocity of the tubes) [15]. However, the rigid-body approximation is expected to be reasonable within the regime of low temperatures and low relative velocities, enough to reduce the dissipation rate. Following the expression obtained by Zheng *et al* [8] for the oscillation frequency which depends on the initial extension of the inner tube as well as on the lengths of the inner and outer tubes, low frequencies, and consequently low relative velocities, can be achieved by just increasing the tube length.

Within these approximations we can write the Hamiltonian of the system as

$$H = \frac{p_1^2}{2m_1} + \frac{p_2^2}{2m_2} + U_{13}(x_1) + U_{23}(x_2) + U_{12}(x_1 - x_2), \quad (1)$$

where m_1 and m_2 are the masses of the core and the inner tube, respectively. The quantities x_1 and x_2 are the separation distances between the centre of mass of the tube (1) and (3) and (2) and (3), respectively, and p_1 (p_2) is the total linear momentum of the core (inner tube). The trajectory of the system at any time t is completely characterized by the four-dimensional set $(x_1(t), p_1(t), x_2(t), p_2(t))$, which is determined by solving the motion equations derived from (1). The potential energy $U = U_{13} + U_{23} + U_{12}$ is due to the excess of van der Waals interaction energy [7, 8], which responds in first order for the main contribution of all the interactions in the system. The potential energy terms can be written in a

compact form as [7, 8]

$$U_{ij}(x_{ij}) = \begin{cases} F_{ij}\, x_{ij}, & \text{if } |L_-| < x_{ij} < L_+ \\ -F_{ij}\, x_{ij}, & \text{if } -|L_+| < x_{ij} < -|L_-| \\ F_{ij}\, |L_-|, & \text{if } x_{ij} \leqslant |L_-| \\ 0, & \text{otherwise,} \end{cases} \quad (2)$$

where $x_{13} = x_1$, $x_{23} = x_2$, $x_{12} = x_1 - x_2$, $L_\pm = (L_i \pm L_j)/2$, F_{ij} is the constant van der Waals force in the tube i due to tube j, and L_i is the length of the tube i.

Two tube configurations were considered. The configuration (**A**) was formed by the following tubes, (1) = (9, 0), (2) = (18, 0), and (3) = (27, 0)[Note 3] and the configuration (**B**) by (1) = (18, 0), (2) = (27, 0), and (3) = (36, 0). The magnitude of the forces for each configuration was estimated from molecular dynamics simulations using the methodology in [9, 10]. The values (in nN) for configuration (**A**) are $F_{12} = 2.5$, $F_{13} = 0.3$, and $F_{23} = 3.5$, and for (**B**) $F_{12} = 3.5$, $F_{13} = 0.4$, and $F_{23} = 4.5$. For the configurations considered in this work we can see that $F_{12}/F_{13} \simeq 8.5$ and $F_{23}/F_{12} \simeq 1.3$. The former value is due to the larger distance between the walls of the tubes (1) and (3) in comparison with tubes (1) and (2) which weakens the van der Waals interactions between those tubes and therefore leads to a smaller value of F_{13}. On the other hand, the latter value is due to the larger diameters of the adjacent tubes (2) and (3) compared with the tubes (1) and (2) (for the same distance between walls $\cong$3.4 Å). These larger diameters increase the number of interacting atoms strengthening the van der Waals interactions between tubes (2) and (3) and therefore making F_{23} greater than F_{12}.

In order to study the influence of the tube length and the length mismatch (e.g. $|L_1 - L_2|$) we have considered different combinations of tube lengths and the corresponding tube masses; the results are presented below. All the quantities in this paper will be written in the following units: length $l_0 = 46.497$ Å, time $t_0 = 1$ ps, mass $m_0 = 1.676 \times 10^{-23}$ kg, momentum $p_0 \equiv m_0 l_0/t_0 = 7.792 \times 10^{-22}$ kg Å ps^{-1}, and energy $E_0 = 93.694$ kcal mol^{-1}.

The evolution of the system was determined by integrating the motion equations derived from (1) through the Hamilton equations:

$$\dot{x_1} = \frac{\partial H}{\partial p_1} = \frac{p_1}{m_1} \quad (3)$$

$$\dot{x_2} = \frac{\partial H}{\partial p_2} = \frac{p_2}{m_2} \quad (4)$$

$$\dot{p_1} = -\frac{\partial H}{\partial x_1} = -(C_{12}(x_{12}) + C_{13}(x_{13})) \quad (5)$$

$$\dot{p_2} = -\frac{\partial H}{\partial x_2} = C_{12}(x_{12}) - C_{23}(x_{23}) \quad (6)$$

where

$$C_{ij}(x_{ij}) = \begin{cases} F_{ij}, & \text{if } |L_-| < x_{ij} < L_+ \\ -F_{ij}, & \text{if } -|L_+| < x_{ij} < -|L_-| \\ 0, & \text{otherwise.} \end{cases} \quad (7)$$

[3] The (N, M) nomenclature is commonly used to classify zigzag ($M = 0$), armchair ($N = M$) and chiral ($N \neq M \neq 0$) nanotubes. The tube diameter is given by $a\sqrt{N^2 + M^2 + NM}/\pi$, where $a = \sqrt{3} \times 1.44$ Å [3].

These four equations were numerically integrated using the fourth-order simplectic method with time step $h = 0.1$ fs [26], i.e., the values of $x_1(t)$, $p_1(t)$, $x_2(t)$, and $p_2(t)$ are given by the succession of the mappings ($i = 1, \ldots, 4$ and $j = 1, 2$):

$$p_j^i = p_j^{i-1} - hc_i \frac{\partial U}{\partial x_j}(x_j^{i-1}), \quad (8)$$

$$x_j^i = x_j^{i-1} + hd_i \frac{\partial T}{\partial p_j}(p_j^i), \quad (9)$$

where T is the kinetic energy, U the potential energy, $x_j(0) = x_j^0$, $p_j(0) = p_j^0$, $x_j(t) = x_j^4$, $p_j(t) = p_j^4$, and c_i and d_i are numerical coefficients[4].

Rivera *et al* [13, 14] studied the motion of a double-walled carbon nanotube oscillator using classical molecular dynamics simulations, and derived a mechanical model similar to the one used in the present work. They included a friction force that opposes the movement of the nanotube in order to reproduce the damped oscillatory behaviour observed in the molecular dynamics results. From their results [14], the friction force was estimated to be more than 40 times smaller than the van der Waals force. The model used in the present work does not include frictional forces, since we are mainly interested in the behaviour of an ideal triple-walled carbon nanotube oscillator system.

In order to characterize the behaviour of the system we have calculated Poincaré sections, i.e., sections in the four-dimensional phase space determined by plotting a point in a $x_1 p_1$ plane each time the trajectory passes through the plane $x_2 = 0$ with $p_2 \geqslant 0$. The section is generated for various initial conditions with the same total energy. Poincaré sections give us the information about the integrability of the system. If the system is integrable, all trajectories appear as a series of points lying on one-dimensional curves and the system is said to be regular. In this case the trajectories are quasiperiodic, developing an orderly pattern over time. On the other hand, if the system is non-integrable, some of the trajectories will appear as a scatter of points limited to a finite region due to energy conservation, thus characterizing a chaotic region.

4. Results

If only the core is allowed to move, the system is reduced to a one-body problem and it is transformed to the usual carbon nanotube oscillator [7]. In this case, the potential energy is given by $U = U_{12} + U_{13}$ with $x_{12} = x_{13} = x_1$, and $x_{23} = 0$ ($U_{23} = 0$) for all times. Figure 3(a) shows the core centre of mass evolution for configuration (**A**), and 3(b) the respective phase space for the above situation. The initial conditions were $x_{10} = 0.5$ and $x_{20} = p_{10} = p_{20} = 0$ ($E = 10$) for $L_1 = 0.94$ and $L_2 = L_3 = 1.0$, and $m_1 = 0.943$, and $m_2 = 1.478$. The flat parts in the phase space (near to $x_1 = 0$) correspond to the situations where the core travels inside the fixed tubes. If the tube lengths are the same (i.e., $L_1 = L_2 = L_3$) these flat regions disappear. The other parts are parabolic and indicate the core motion during the action of the constant van der Waals force due to the fixed

[4] The values of the coefficients are given by [26]: $c_1 = c_4 = \alpha + \frac{1}{2}$, $c_2 = c_3 = -\alpha$, $d_1 = d_3 = 2\alpha + 1$, $d_2 = -4\alpha - 1$, and $d_4 = 0$, where $\alpha \cong 0.1756$.

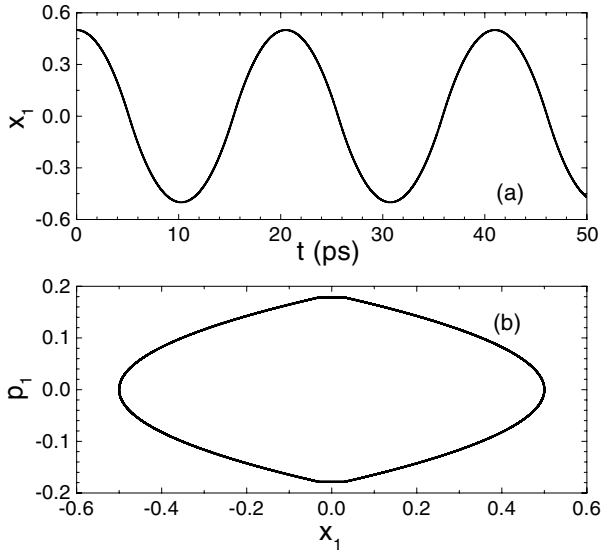

Figure 3. (a) Evolution of the core centre of mass for the case where both inner and outer tubes are kept fixed and (b) the respective phase space.

tubes. For these conditions, we recover the main features of the previous results [8, 7, 9] for the oscillatory core movement and, for the particular configuration used here, with an oscillation frequency of approximately 49 GHz (see the complementary material, movie 1, at stacks.iop.org/Nano/16/583).

If we also allow the movement of the inner tube, the resulting configuration is converted to a coupled oscillator system and is described by the Hamiltonian (1) within the rigid-body approximation. We have found that, in this case, the system exhibits a mixed behaviour, partly chaotic and partly regular, which is due to the interaction between the core (1) and the inner tube (2). In our case this interaction is controlled by F_{12}, which is determined by the tube configuration. In order to see the role of this interaction in the chaotic signature, different values were assigned to F_{12}. The resulting dynamics are presented in figure 4, which shows the Poincaré sections for configuration (**B**) with $L_1 = L_2 = L_3 = 10$ and $m_1 = 14.78$ and $m_2 = 19.71$ for $E = 14.64$. When the interaction is very weak (figure 4(a)) the system presents a regular character, but as F_{12} is increased to its maximum allowed value, chaotic behaviour emerges (figures 4(b)–(d)). In this case, chaotic and regular regions co-exist, and the system is characterized by presenting a soft deterministic chaos [18, 19].

Another quantity that affects the dynamics of the system is the relation between the moveable tube lengths. This is illustrated in figure 5, where we present Poincaré sections for configuration (**A**) for different tube lengths. When the lengths are equal (figures 5(a) and (c)), the same type of dynamics is present even when the total energy of the system is altered. This result indicates that when the lengths of all tubes that compose the oscillator are equal the Hamiltonian (1) is invariant under a scale transformation. This property can be seen in several other types of potentials (see for instance [27]). This scale invariance allows us to make predictions about tubes with large lengths simulating tubes with small lengths, which is the case presented here.

On the other hand, when $L_1 \neq L_2$ and $L_2 = L_3$ the picture is different. In this case (figures 5(b) and (d)), the scale invariance of the Hamiltonian is broken, and distinct dynamics appear and the dependence on the total energy is evident.

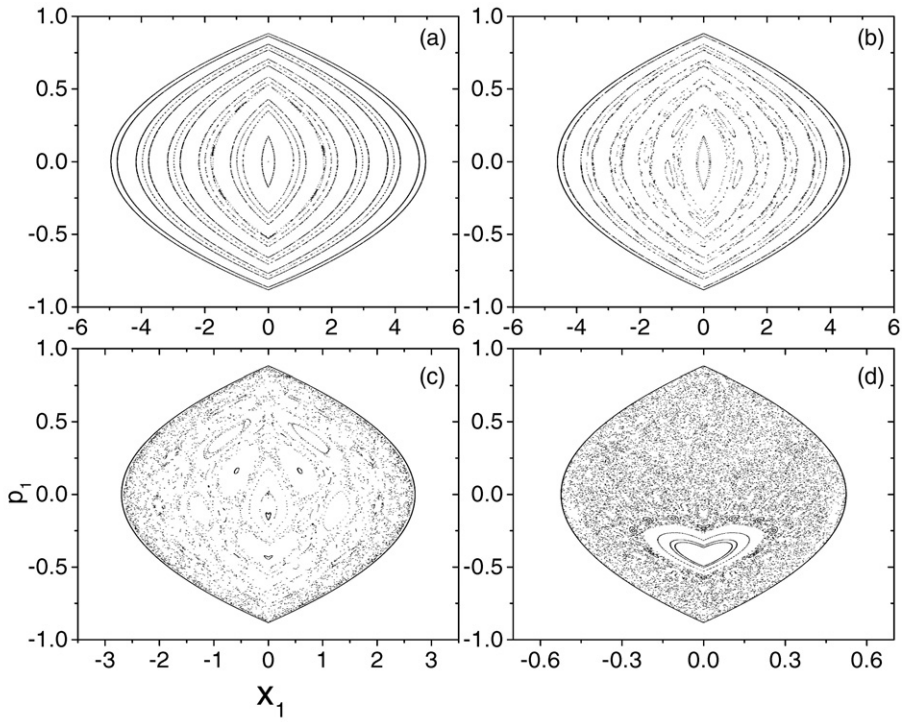

Figure 4. Resulting Poincaré sections of the system where both core and inner tube can move (configuration (**B**)) for different values of F_{12} (in nN): (a) 0.0035, (b) 0.035, (c) 0.35, and (d) 3.5.

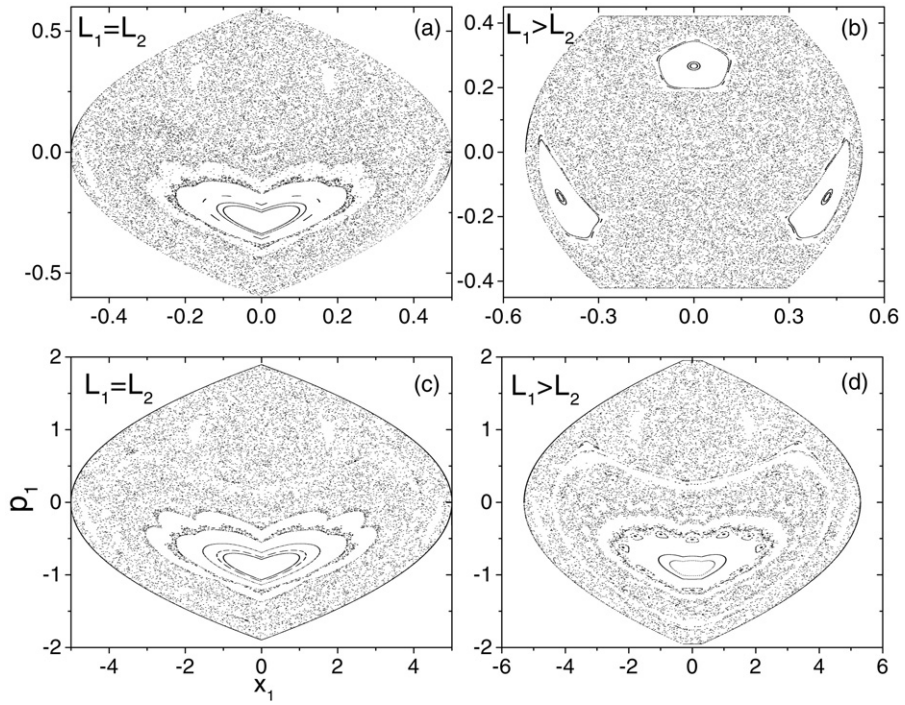

Figure 5. Resulting Poincaré sections of the evolution of configuration (**A**) for (a) $E = 100$, (b) $E = 106$, (c) $E = 10$, and (d) $E = 10.6$. The tube lengths used were: ((a), (c)) $L_1 = L_2 = L_3 = 10$, and ((b), (d)) $L_1 = 10.6$, and $L_2 = L_3 = 10$.

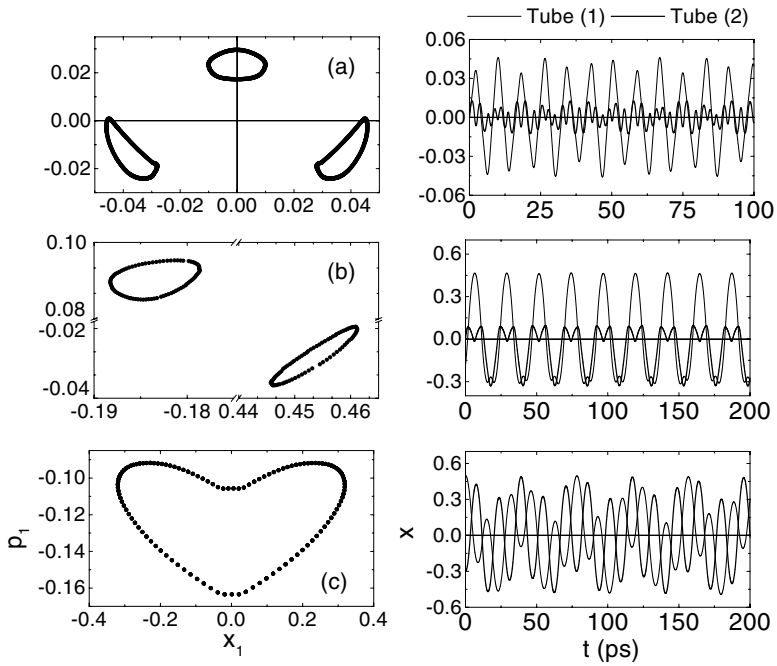

Figure 6. Poincaré sections showing examples of regular orbits found in three total energy values: (a) $E = 1$, (b) $E = 10$, and (c) $E = 23$, respectively. Configuration (**A**) was used in this case with lengths $L_1 = 0.94$ and $L_2 = L_3 = 1.0$. The respective centre of mass motion for each case is shown on the right side of the figure.

In both figures 4 and 5 we can see chaotic regions permeating islands of regularity. The pattern and distribution of the islands size depend on the total energy. For the particular cases of figures 4(d) and 5(c) we can observe a 'heart'-shaped region. The presence of these one-dimensional curves indicates the existence of stable quasiperiodic orbits when specific initial conditions are chosen. This aspect is illustrated in figure 6, where three selected regular orbits are shown. In figure 6(a) both tubes oscillate with small amplitudes, with the inner tube showing the smaller one. For a higher energy (figure 6(b)) the amplitudes are increased and the oscillation pattern is different. For this situation, the core reaches both right and left sides of the oscillator, while the range of the inner tube oscillation is comprised mainly in the left side (see the complementary material, movies 2 and 3, at stacks.iop.org/Nano/16/583).

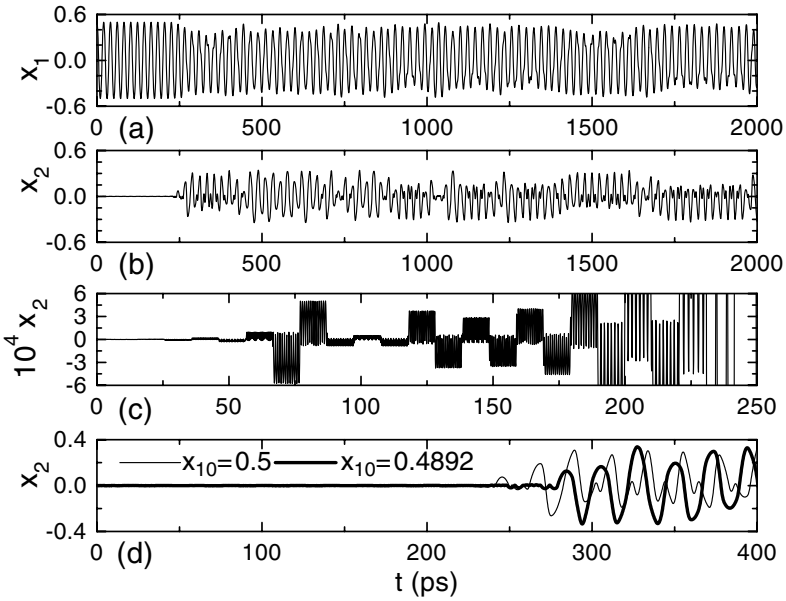

Figure 7. Example of a chaotic behaviour presented by (a) the core and (b) the inner tube. The initial conditions were $x_{10} = 0.5$ and $x_{20} = p_{10} = p_{20} = 0$ ($E = 10$). In (c) the graph presents the behaviour of inner tube at the first 250 ps of the movement. In (d) the inner tube motion is shown for two slightly different initial conditions $x_{10} = 0.5$ (=23.248 Å) and $x_{10} = 0.4892$ (=22.746 Å), with $x_{20} = p_{10} = p_{20} = 0$ in both cases.

In figure 6(c) the selected 'heart'-shaped orbit is shown; this was obtained by setting $x_{10} = 0.5$, $x_{20} = -0.3$, and $p_{10} = p_{20} = 0$, i.e., the tubes are extruded in opposite directions and then released. For this situation, the amplitudes are comparable and the movements of both tubes are approximately the same up to a phase shift (see movie 4, at stacks.iop.org/Nano/16/583). Interestingly, the Poincaré sections showing 'heart'-shaped curves (figure 4(d) for instance) are very similar to the one found near to a nonlinear resonance island for the driven one-dimensional hydrogen system [22]. Quasiperiodic orbits have also been reported by Sohlberg *et al* when the movement of molecular bearings has been investigated using rigid-body dynamics [25]. As pointed out by Sohlberg *et al*, these types of trajectories are important because they correspond to frictionless motion. In the case of oscillators we remark that the quasiperiodic orbits are dependent on the initial conditions, and that perturbations can produce chaotic results.

An example of a chaotic movement is shown in figures 7(a)–(c), obtained for configuration (**A**) ($L_1 = 0.94$ and $L_2 = L_3 = 1.0$) from the condition where the core was released from the rest (zero initial velocity) at the position $x_{10} = 0.5$, and the inner tube was initially at rest at $x_{20} = 0$ ($E = 10$). Small oscillations of high frequency are induced in the inner tube by the core during the first 250 ps (figure 7(c)). After this period, the oscillation amplitude of the inner tube increases and its movement begins to disturb the core motion more strongly (see the complementary material, movie 5, at stacks.iop.org/Nano/16/583). The resulting orbit presents chaotic features and therefore no periodicity is observed. In addition, the system evolution is very sensitive to changes in the initial conditions when they are in a chaotic phase space region. This is illustrated in figure 7(d), where we have changed the releasing point x_{10} by 0.5 Å and have obtained a totally different inner tube evolution after about 250 ps. Such sensitivity makes the behaviour of the analysed coupled carbon nanotube oscillator unpredictable over longer timescales.

Despite the presence of chaotic regions, the existence of regular orbits could allow the development of multi-functional nano-devices. Choosing and setting appropriate initial conditions for a carbon nanotube oscillator ($n > 2$ and $k \geqslant 1$), different motion types could be provided by the device. Each type could represent a specific role within a nanomachinery context, thus providing operational building blocks for nanomechanical systems in the sense of the scheme proposed by Kang and Hwang [17]. However, temperature and energy dissipation effects must be carefully considered and investigated, since they can lead to undesirable device behaviours.

5. Conclusion

We investigated configurations of MWNT nano-oscillators composed of three tubes where the outer one is fixed and both core and inner tube are allowed to move. Through rigid-body dynamics simulations we found typical signatures of soft deterministic chaos, where chaotic and regular regions co-exist. This is the first indication of chaos in nanoscaled mechanical systems based on multiwalled carbon nanotube oscillators [7]. The regular orbits can be tuned by varying the total energy of the system, e.g., by releasing the extruded core and inner tube from the rest in different initial positions. Appropriately choosing the initial conditions can provide a way to induce different movements of the coupled oscillators, thus allowing the construction of a multi-functional nano-device based on MWNT oscillators. Besides the technological interest in these systems, the addition of a fourth nanotube, heavier and slower, could provide a very interesting system to study adiabatic energy dissipation induced by chaos [28, 29]. Work along this direction is in progress.

Acknowledgments

We thank Marcus V S Bonança for useful discussions and acknowledge the Brazilian Agency FAPESP for the financial support.

References

[1] Iijima S 1991 *Nature* **354** 56
[2] Baughman R H, Zakhidov A A and de Heer W A 2002 *Science* **297** 787
[3] Sinnott S B and Andrews R 2001 *Crit. Rev. Solid State Mater. Sci.* **26** 145 and references therein
[4] Rinzler A G, Hafner J H, Nikolaev P, Lou L, Kim S G, Tomanek D, Nordlander P, Colbert D T and Smalley R E 1995 *Science* **269** 1550
[5] Tans S J, Devoret M H, Dal H, Thess A, Smalley R E, Geerligs L J and Dekker C 1997 *Nature* **386** 474
[6] Cumings J and Zettl A 2000 *Science* **289** 602
[7] Zheng Q and Jiang Q 2002 *Phys. Rev. Lett.* **88** 045503
[8] Zheng Q, Liu J Z and Jiang Q 2002 *Phys. Rev.* B **65** 245409
[9] Legoas S B, Coluci V R, Braga S F, Coura P Z, Dantas S O and Galvão D S 2003 *Phys. Rev. Lett.* **90** 055504
[10] Legoas S B, Coluci V R, Braga S F, Coura P Z, Dantas S O and Galvão D S 2004 *Nanotechnology* **15** S184
[11] Guo W, Guo Y, Gao H, Zheng Q and Zhong W 2003 *Phys. Rev. Lett.* **91** 125501
[12] Zhao Y, Ma C-C, Chen G and Jiang Q 2003 *Phys. Rev. Lett.* **91** 175504
[13] Rivera J L, McCabe C and Cummings P T 2003 *Nano Lett.* **3** 1001
[14] Rivera J L, McCabe C and Cummings P T 2005 *Nanotechnology* **16** 186
[15] Tangney P, Louie S G and Cohen M L 2004 *Phys. Rev. Lett.* **93** 065503
[16] Kang J W and Hwang H J 2004 *J. Appl. Phys.* **96** 3900
[17] Kang J W and Hwang H J 2004 *Nanotechnology* **15** 1633
[18] Ott E 1993 *Chaos in Dynamical Systems* (Cambridge: Cambridge University Press)
[19] Gutzwiller M C 1990 *Chaos in Classical and Quantum Mechanics* (New York: Springer)
[20] Jensen R V 1982 *Phys. Rev. Lett.* **49** 1365
[21] Jensen R V 1984 *Phys. Rev.* A **30** 386
[22] Jensen R V 1987 *Phys. Scr.* **35** 668
[23] Burnell F, Mann R B and Ohta T 2003 *Phys. Rev. Lett.* **90** 134101
[24] Bacsa R R, Laurent C, Peigney A, Bacsa W S, Vaugien T and Rousset A 2000 *Chem. Phys. Lett.* **323** 566
[25] Sohlberg K, Tuzun R E, Sumpter B G and Noid D W 1997 *Nanotechnology* **8** 103
[26] Forest E and Ruth R 1990 *Physica* D **43** 105
Yoshida H 1990 *Phys. Lett.* A **150** 262
[27] Carnegie A and Percival I C 1984 *J. Phys. A: Math. Gen.* **17** 801
[28] Berry M V and Robbins J M 1993 *Proc. R. Soc.* A **442** 659
[29] Auslaender O M and Fishman S 2000 *Phys. Rev. Lett.* **84** 1886